International Symposium
On Turbulence and Shear Flow
Phenomena (TSFP-9)
June 30 - July 3, 2015 *Melbourne, Australia*

CONDITIONAL FLOW STATISTICS AND ALIGNMENT OF PRINCIPAL STRAIN RATES, VORTICITY, AND SCALAR GRADIENTS IN A TURBULENT NONPREMIXED JET FLAME

Antonio Attili
Clean Combustion Research Center
King Abdullah University of Science and Technology
Thuwal, Saudi Arabia
antonio.attili@kaust.edu.sa

Fabrizio Bisetti
Clean Combustion Research Center
King Abdullah University of Science and Technology
Thuwal, Saudi Arabia
fabrizio.bisetti@kaust.edu.sa

ABSTRACT

The alignment of vorticity and gradients of conserved and reactive scalars with the eigenvectors of the strain rate tensor (i.e., the principal strains) is investigated in a direct numerical simulation of a turbulent nonpremixed flame achieving a Taylor's scale Reynolds number in the range $100 \leq \mathrm{Re}_\lambda \leq 150$ (Attili *et al.* Comb. Flame, 161, 2014). The vorticity vector displays a pronounced tendency to align with the direction of the intermediate strain. These alignment statistics are in almost perfect agreement with those in homogeneous isotropic turbulence (Ashurst *et al.* Physics of Fluids 30, 1987) and differ significantly from the results obtained in other nonpremixed flames in which vorticity alignment with the most extensive strain was observed (Boratav *et al.* Physics of Fluids 8, 1996). The gradients of conserved and reactive scalars align with the most compressive strain. It is worth noting that conditioning on the local values of the mixture fraction, or equivalently conditioning on the distance from the flame sheet, does not affect the statistics. Our results suggest that turbulence overshadows the effects of heat release and chemical reactions. This may be due to the larger Reynolds number achieved in the present study compared to that in previous works.

INTRODUCTION

Understanding the interaction between strain rate and scalar gradients (i.e., scalar dissipation rate) is critical to the modeling of turbulent flames as scalar dissipation affects chemical reaction strongly. In addition, RANS and LES combustion models often rely on closure strategies developed in the framework of incompressible turbulence; therefore, it is important to characterize the effects of heat release and hydrodynamic-combustion interactions on the small scale features of turbulence. The principal components of the strain rate tensor are computed with the eigendecomposition of the tensor. The three eigenvalues $\alpha > \beta > \gamma$ of the strain rate tensor are the principal strains and the corresponding eigenvectors identify the direction of the three principal strains. In the case of isotropic turbulence, Ashurst *et al.* (1987) showed that the vorticity vector tends to align with the intermediate principal strain β, while the passive scalar gradient aligns preferentially with the most compressive strain γ and is perpendicular to the intermediate strain; therefore, scalar dissipation occur predominantly in sheet-like structures whose normal is aligned perpendicularly to the most compressive strain. These observations for isotropic turbulence have been confirmed by many studies. In addition, the most probable values of the three principal strains have been found to be in the ratio $3:1:-4$ (the sum must be zero in incompressible flow) (Ashurst *et al.*, 1987). In the past, it has been reported that the alignment statistics in turbulent flames show significant deviation from incompressible isothermal flows. Nomura & Elghobashi (1993) and Boratav *et al.* (1996) showed that the dominance of strain over vorticity in DNS of turbulent low-Reynolds number flames causes the alignment of vorticity with the α-strain, in contrast with the β-strain/vorticity alignment in constant density flows. Boratav *et al.* (1998) extended this study conditioning the result on the value of mixture fraction Z. They found β-strain/vorticity alignment in the fuel ($Z \to 1$) and oxidizer ($Z \to 0$) regions and α-strain/vorticity alignment in region of mixture fraction around stoichiometry, characterized by significant heat release. The conserved scalar gradient (i.e., mixture fraction) shows a clear alignment with the most compressive γ-strain in isotropic turbulence as well as in nonpremixed (Boratav *et al.*, 1998) and premixed (Malkeson & Chakraborty, 2011) flames. However, Malkeson & Chakraborty (2011) showed that the gradient of a reactive scalar (the fuel mass fraction) aligns with the most extensive α-strain when chemical reactions overshadow the effect of turbulence.

In the present study, the alignment of vorticity and gradients of conserved (mixture fraction) and reactive (temperature and naphthalene mass fraction) scalars with the eigenvectors of the strain rate tensor (i.e., principal strains)

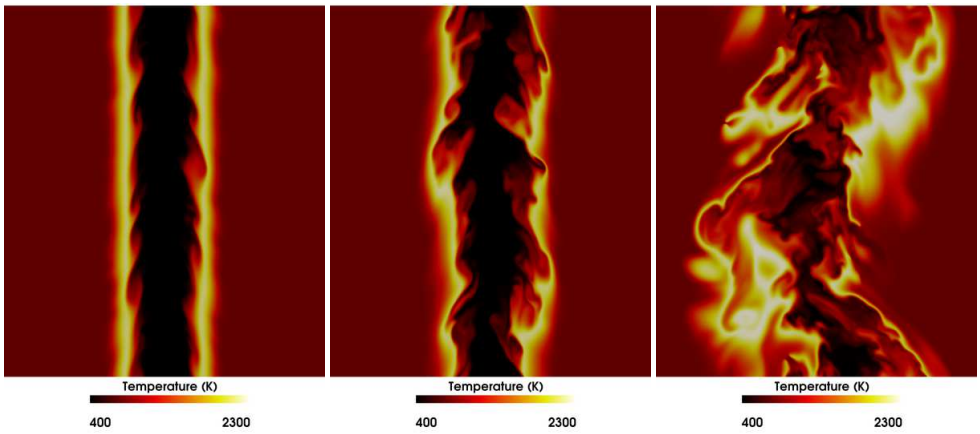

Figure 1. Two-dimensional cut of the temperature field at three different times. Only the central part of the domain in the crosswise direction is shown.

is investigated in a DNS of turbulent nonpremixed flame achieving a Taylor's scale Reynolds number in the range $100 \leq \mathrm{Re}_\lambda \leq 150$ (Attili *et al.*, 2014; Bisetti *et al.*, 2014; Attili *et al.*, 2015). The naphthalene mass fraction has been selected because it is characterized by a strong sensitivity to the local flow condition due to its slow chemistry (Attili *et al.*, 2014); in addition, it has negligible effects on the hydrodynamics.

CONFIGURATION AND METHODS

Three-dimensional, temporally-evolving turbulent nonpremixed planar jet flames are considered (Attili *et al.*, 2014). The fuel jet is *n*-heptane diluted in 85% nitrogen at 400 K and is surrounded by air at 800 K, yielding a stoichiometric mixture fraction $Z_{\mathrm{st}} = 0.147$. The pressure is atmospheric. The gas phase hydrodynamics are modeled with the reactive Navier-Stokes (N-S) equations in the low Mach number limit. The transport of heat and mass is described using the Hirschfelder and Curtiss approximation to the diffusive fluxes and all properties are computed with a mixture-average approach (Attili *et al.*, 2014). Combustion is modeled using a detailed chemical mechanism for the oxidation of *n*-heptane comprising 47 species and 290 reactions (Bisetti *et al.*, 2012).

The flow is periodic in the streamwise (x) and spanwise (z) directions and open boundary conditions are prescribed in the crosswise direction (y). A realization of a fully developed turbulent channel flow at $\mathrm{Re}_\tau = 390$ is used to initialize the velocity field in the fuel core. The mean axial velocity on the jet centerline ($y/H = 0$) is $U_c = 8.74$ m/s and the air coflow velocity is $U_{co} = -8.74$ m/s. The jet Reynolds number is $(U_c - U_{co})H/\nu \approx 15000$. The domain spans $L_x = 9.4$, $L_y = 10.5$, and $L_z = 4.7$ cm and is discretized with $1024 \times 1024 \times 512 \approx 500$ million points. The mesh size h results in a spatial resolution below the minimum average Kolmogorov scale ($\eta = 110$ μm and $h/\eta \approx 0.82$) and the thin reaction fronts are adequately resolved.

An overview of the flowfield evolution is shown in Fig. 1 using a two-dimensional cut of the temperature field at three different time instants. Two twin non-premixed flames develop in the region of high turbulence production. The velocity field resulting from the Kelvin-Helmholtz instabilities and the subsequent turbulent motion wrinkle and stretch the flames. In the second half of the simulation time, the flow and temperature fields are characterized by complex flow structures and by the simultaneous presence of very different length scales.

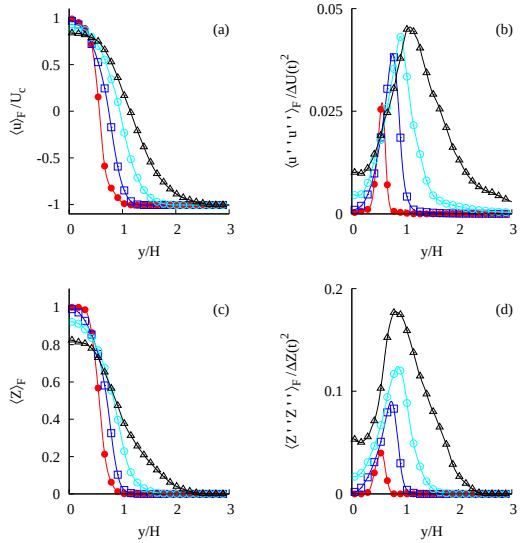

Figure 2. Favre-averaged statistics at several time instants: 5 ms (filled circles), 10 ms (squares), 15 ms (open circles), and 20 ms (triangles). Mean (a) and variance (b) of the streamwise velocity; mean (c) and variance (d) of mixture fraction. The crosswise coordinate y is scaled with the initial jet thickness H. The mean velocity is scaled with the initial centerline velocity U_c and the velocity variance with the instantaneous mean velocity difference between the center of the jet and the coflow $\Delta U(t) = \langle U(y=0,t)\rangle_{\mathrm{F}} - U(y \to \pm\infty)$, where $U(y \to \pm\infty) = -U_c$. The mixture fraction variance is scaled with $\Delta Z(t) = \langle Z(y=0,t)\rangle_{\mathrm{F}} - Z(y \to \pm\infty)$, where $Z(y \to \pm\infty) = 0$.

Favre-averaged statistics of the streamwise velocity and mixture fraction are shown in Fig. 2 at several time instants. The Favre average of the field ϕ is defined as $\langle\phi\rangle_{\mathrm{F}} = \langle\rho\phi\rangle / \langle\rho\rangle$, where the angular brackets indicate an

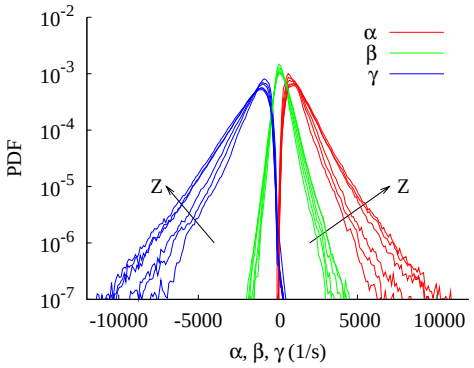

Figure 3. Probability density functions of the three eigenvalues of the strain rate tensor α (red), β (green), and γ (blue). Each line represents a different value for the conditioning variable Z: 0.1, 0.147, 0.17, 0.3, 0.55, 0.8.

average in the streamwise and spanwise directions and the fluctuations ϕ'' are defined with respect to the Favre average: $\phi'' = \phi - \langle\phi\rangle_{\rm F}$.

RESULTS

Probability density functions of the three eigenvalues of the strain rate tensor α, β, and γ, conditioned on different values of mixture fraction, are shown in Fig. 3. The conditioning values are: 0.1 (lean side of the flame), 0.147 (stoichiometry), 0.17 (mixture fraction at peak temperature), 0.3 (mixture fraction at peak naphthalene), 0.55 and 0.8 (rich mixture fraction). The PDFs are characterize by wide exponential tails due to the intermittency of the velocity gradient. The α-strain (most extensive) is alway positive, while the γ-strain is characterize by the existence of a non-zero, albeit small, probability of positive value. In this case the three principal strains are all positive (extensive) due to the effect of heat release on the velocity divergence as the sum of the principal strains is equal to the velocity divergence. This does not occur in constant density flows due to the divergence being zero. The PDFs display a weak dependence on the conditional value of mixture fraction, with a slight increase in the variance at larger Z. The most probable values of the three eigenvalues are in the ratio $6.5:1:-6.5$, different from that for constant density flow: $3:1:-4$. The value of the ratio observed in the present flame are in good agreement with the measurement reported by Gamba *et al.* (2013) in the far field of a turbulent nonpremixed jet flame.

Figure 4 shows the alignment statistics of the eigenvectors of the strain rate tensor, i.e., direction of the principal strains, with the vorticity vector. The same statistics for the homogeneous isotropic turbulence simulation of Ashurst *et al.* (1987) are also shown. The vorticity vector displays a tendency to align with the direction of the intermediate strain e_β. The probability of vorticity to be perpendicular to the most compressive strain is found also. It is apparent that there is no preferential alignment of the vorticity vector in the direction of the α-strain. The results are independent with respect to the conditioning on mixture fraction. These alignment statistics between vorticity and strain are in almost perfect agreement with that of homogeneous isotropic turbulence (Ashurst *et al.*, 1987) and differ significantly from the results obtained in other nonpremixed flames in which the α-strain/vorticity alignment

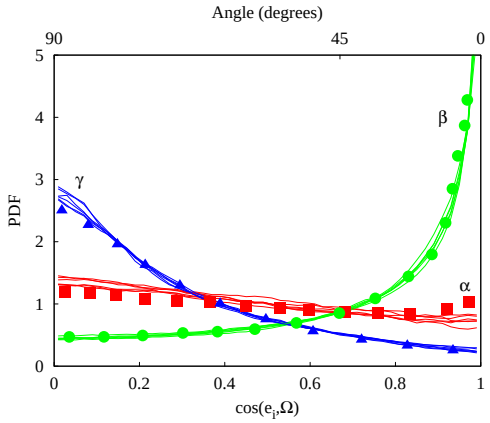

Figure 4. Probability density functions of the cosine of the angle between the direction of the principal strains e_α (red lines), e_β (green lines), and e_γ (blue lines) and the direction of vorticity in the turbulent flame DNS. Each line represents a different value for the conditioning variable Z: 0.1, 0.147, 0.17, 0.3, 0.55, 0.8. Symbols show the same statistics for the homogeneous isotropic turbulence simulation of Ashurst *et al.* (1987).

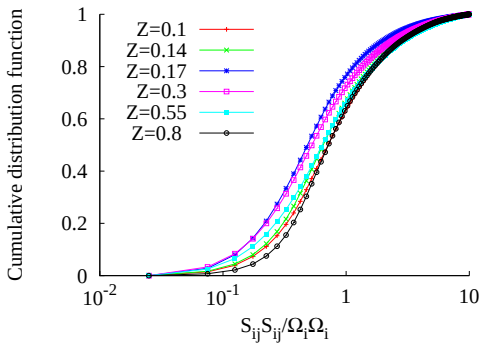

Figure 5. Cumulative distribution function of the ratio between strain and vorticity magnitudes at different mixture fractions.

was observed (Boratav *et al.*, 1996).

Boratav *et al.* (1996) explain that the alignment of vorticity with the α-strain in flame is induced by the dominance of strain over vorticity. This phenomenon is present in incompressible flows also, but occurs with relatively low probability (Dresselhaus & Tabor, 1992). Statistics of the ratio between strain and vorticity magnitude are shown in Fig. 5 for the present flame. For all the conditioning values of mixture fraction, the volume of fluid characterized by the dominance of vorticity over strain is larger that that characterized by the opposite case. In particular, for 65 to 80% of the points the vorticity magnitude is larger than the strain magnitude, depending on mixture fraction. We speculate that the differences between the flame described by Boratav *et al.* (1996) and the present case are related to the much larger Reynolds number achieved in the latter.

Alignment statistics between strain and the gradient of selected scalars are shown in Figs. 6 and 7. Three scalars are considered: *(i)* mixture fraction, a conserved passive

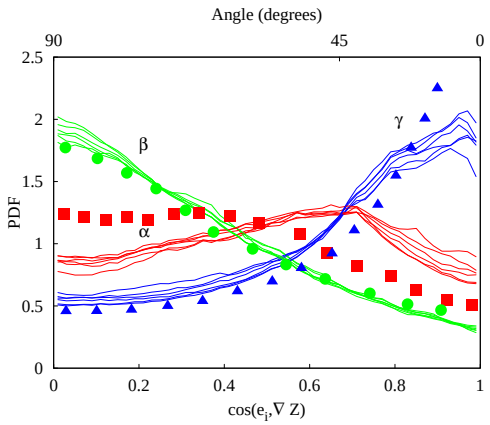

Figure 6. Probability density functions of the cosine of the angle between the direction of the principal strains e_α (red lines), e_β (green lines), and e_γ (blue lines) and the direction of the mixture fraction gradient in the turbulent flame DNS. Each line represents a different value for the conditioning variable Z: 0.1, 0.147, 0.17, 0.3, 0.55, 0.8. Symbols show the same statistics for the homogeneous isotropic turbulence simulation of Ashurst *et al.* (1987).

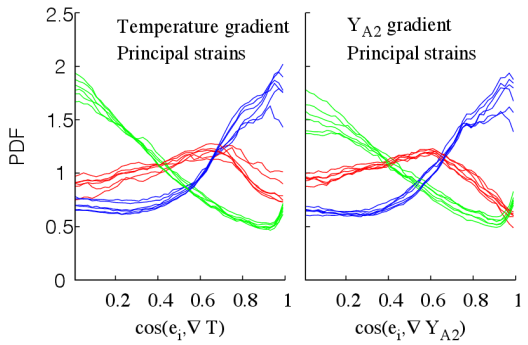

Figure 7. Probability density functions of the cosine of the angle between the direction of the principal strains e_α (red), e_β (green), and e_γ (blue) and the direction of reactive scalar gradients (temperature and naphthalene, Y_{A2} mass fraction). Each line represents a different value for the conditioning variable Z: 0.1, 0.147, 0.17, 0.3, 0.55, 0.8.

scalar; *(ii)* temperature, a reactive and active scalar that affects the fluid density, viscosity, and velocity field; *(iii)* naphthalene mass fraction, a reactive scalar that is very sensitive to the local scalar dissipation and strain fields, but has a negligible influence on the flame hydrodynamics (Attili *et al.*, 2014). Figure 6 shows also the results for homogeneous isotropic turbulence (Ashurst *et al.*, 1987). It is evident that the gradient of all the three scalars aligns with strain in the same way and the result is also independent of mixture fraction. All gradients align with the γ-strain, that is mostly compressive (see Fig. 3), are perpendicular to the intermediate strain, and tends to be at 45 degrees with respect to the most extensive strain. Similarly to the case of vorticity, this results are very similar to the case of incompressible turbulence. We conclude that the statistics of alignment are not sensitive to heat release in the present turbulent flame and do not change whether the scalar is active (temperature) or sensitive to the hydrodynamics due to its slow chemistry (naphthalene).

CONCLUSION

Alignment statistics of vorticity and scalar gradients with respect to the principal axis of the strain rate tensor are analyzed in a turbulent nonpremixed jet flames. The analysis clearly shows that the alignment statistics in the turbulent flame agree with those observed in constant-density homogeneous isotropic turbulence. In addition, conditioning on the local values of the mixture fraction does not affect the statistics. As our results contradict previous studies, we speculate that the effects of heat release and chemical reactions are completely overshadowed by turbulence in the present case. This is perhaps due to the larger Reynolds number achieved in the present study compared to that in previous works.

REFERENCES

Ashurst, Wm. T., Kerstein, A. R., Kerr, R. M. & Gibson, C. H. 1987 Alignment of vorticity and scalar gradient with strain rate in simulated Navier–Stokes turbulence. *Physics of Fluids* **30** (8), 2343–2353.

Attili, A., Bisetti, F., Mueller, M. E. & Pitsch, H. 2014 Formation, growth, and transport of soot in a three-dimensional turbulent non-premixed jet flame. *Combustion and Flame* **161**, 1849–1865.

Attili, A., Bisetti, F., Mueller, M. E. & Pitsch, H. 2015 Damköhler number effects on soot formation and growth in turbulent nonpremixed flames. *Proceedings of the Combustion Institute* **35**, 1215–1223.

Bisetti, F., Attili, A. & Pitsch, H. 2014 Advancing predictive models for particulate formation in turbulent flames via massively parallel direct numerical simulations. *Philosophical Transactions of the Royal Society* **372** (2022), 20130324.

Bisetti, F., Blanquart, G., Mueller, M. E. & Pitsch, H. 2012 On the formation and early evolution of soot in turbulent nonpremixed flames. *Combustion and Flame* **159** (1), 317–335.

Boratav, O. N., Elghobashi, S. E. & Zhong, R. 1996 On the alignment of the α-strain and vorticity in turbulent nonpremixed flames. *Physics of Fluids* **8** (8), 2251–2253.

Boratav, O. N., Elghobashi, S. E. & Zhong, R. 1998 On the alignment of strain, vorticity and scalar gradient in turbulent, buoyant, nonpremixed flames. *Physics of Fluids (1994-present)* **10** (9), 2260–2267.

Dresselhaus, E. & Tabor, M. 1992 The kinematics of stretching and alignment of material elements in general flow fields. *Journal of Fluid Mechanics* **236**, 415–444.

Gamba, M., Clemens, N. T. & Ezekoye, O. A. 2013 Volumetric PIV and 2D OH PLIF imaging in the far-field of a low Reynolds number nonpremixed jet flame. *Measurement Science and Technology* **24** (2), 024003.

Malkeson, S. P. & Chakraborty, N. 2011 Alignment statistics of active and passive scalar gradients in turbulent stratified flames. *Physical Review E* **83** (4), 046308.

Nomura, K. K. & Elghobashi, S. E. 1993 The structure of inhomogeneous turbulence in variable density nonpremixed flames. *Theoretical and Computational Fluid Dynamics* **5** (4-5), 153–175.